Published in final edited form as:
Cancer Res. 2012 April 1; 72(7): 1728–1739. doi:10.1158/0008-5472.CAN-11-2762.

RORα suppresses breast tumor invasion through inducing SEMA3F expression

Gaofeng Xiong[1], **Chi Wang**[1], **B. Mark Evers**[1,3], **Binhua P. Zhou**[1,4], and **Ren Xu**[1,2]

[1]Markey Cancer Center University of Kentucky, Lexington, KY 40536, USA

[2]Department of Molecular and Biomedical Pharmacology, University of Kentucky, Lexington, KY 40536, USA

[3]Department of Surgery, University of Kentucky, Lexington, KY 40536, USA

[4]Department of Molecular and Cellular Biochemistry, University of Kentucky, Lexington, KY 40536, USA

Abstract

Inactivation of tumor suppressors and inhibitory microenvironmental factors is necessary for breast cancer invasion; therefore, identifying those suppressors and factors is crucial not only to advancing our knowledge of breast cancer, but also to discovering potential therapeutic targets. By analyzing gene expression profiles of polarized and disorganized human mammary epithelial cells (HMECs) in a physiologically relevant three-dimensional (3D) culture system, we identified retinoid orphan nuclear receptor alpha (RORα) as a transcription regulator of semaphorin 3F (SEMA3F), a suppressive microenvironmental factor. We showed that expression of RORα was down-regulated in human breast cancer tissue and cell lines, and that reduced mRNA levels of RORα and SEMA3F correlated with poor prognosis. Restoring RORα expression reprogrammed breast cancer cells to form non-invasiveness structures in 3D culture and inhibited tumor growth in nude mice, accompanied by enhanced SEMA3F expression. Inactivation of RORα in non-malignant HEMCs inhibited SEMA3F transcription and impaired polarized acinar morphogenesis. Using chromatin immunoprecipitation and luciferase reporter assays, we showed that transcription of SEMA3F is directly regulated by RORα. Knockdown of SEMA3F in RORα-expressing cancer cells rescued the aggressive 3D phenotypes and tumor invasion. These findings indicate that RORα is a potential tumor suppressor and inhibits tumor invasion by inducing suppressive cell microenvironment.

Keywords

Orphan nuclear receptor; microenvironment; breast cancer; cell polarity; invasion

Introduction

The nuclear receptor superfamily contains a number of orphan receptors for which no ligand has been well characterized. Retinoid orphan nuclear receptor alpha (RORα) is a member of the orphan nuclear factor family and regulates gene expression by binding to ROR response elements (ROREs) (1, 2). Expression of RORα has been detected in multiple tissues and

Address correspondence to: Ren Xu, Ph.D. Department of Molecular and Biomedical Pharmacology University of Kentucky, BBSRB 741 S. Limestone Lexington, KY 40536 USA ren.xu20101@uky.edu Phone: 859-3237889 Fax: 859-2576030.

No conflicts of interest to be disclosed.

cells including brain, heart, skin, muscle, colon, lung, spleen, leukocytes, and mammary epithelial cells (1, 3–7). This factor regulates various cell functions including differentiation, metabolism, inflammation, transformation, and circadian clock function (6, 8–10). The RORα gene maps to 15q22.2, a region that is often deleted in cancer, thus RORα has been proposed to be inactivated during cancer development (11). One recent study showed that phosphorylated RORα attenuates transcriptional activity of β-catenin and inhibits anchorage independent growth of colon cancer cells, suggesting that RORα is a potential tumor suppressor in colon cancer (6). However, the function of RORα in breast cancer development and progression largely is unknown.

Mammary tissue morphogenesis and differentiation is controlled by various microenvironmental cues, including secretory factors, cell-extracellular matrix (ECM) and cell-cell contacts, as well as their downstream signals (12, 13). These microenvironmental signals are often dysregulated during breast cancer development and progression, leading to disruption of tissue polarity, enhanced cell invasion and metastasis (14–16). To investigate how the microenvironmental cues contribute to breast cancer progression, Dr. Bissell's laboratory developed a 3D culture model using HMT-3522 human breast cancer progression cell lines (S1, T4-2) (17). It has been shown that non-malignant mammary epithelial cells maintain acinar structures and tissue specific function in 3D culture (18–20), while malignant cells form proliferative and invasive structures, which mimics the *in vivo* phenotypes of normal and tumor cells. These results indicate that 3D culture model is more physiologically relevant to study function and structure of malignant and non-malignant mammary epithelial cells. In 3D culture model, the non-malignant S1 cells form polarized spheroids, while their malignant counterpart T4-2 cells form disorganized structures. Furthermore, blocking β1-integrin, EGFR, or MMP pathways reprograms T4-2 cells to form polarized and non-invasive acini-like structures (reverted T4-2) (20–22). By analyzing the gene expression profiles of S1, T4-2 and reverted T4-2 cells in 3D culture, we have identified many microenvironment-related genes that are differentially expressed in polarized and disorganized cells, including SEMA3F.

SEMA3F is one of the microenvironmental factors with tumor suppressor function. This protein was first identified as a repulsive factor of axon guidance in neuron development by modulating cell polarization and migration (23, 24). Expression of SEMA3F in cancer cells inhibits tumor growth, invasion, and metastasis through binding to its receptor, neuropilin 1 (NRP1) and NRP2 (25, 26). SEMA3F can also inhibit tumor angiogenesis by acting directly on vascular endothelial cells via NRP2 (27). Thus, SEMA3F has been considered a potential therapeutic target that has the advantage of inhibiting both tumor cells and endothelial cells. Inactivation of SEMA3F during cancer development has been attributed to genomic instability, because the SEMA3F gene locates at chromosome 3p21.3, which is commonly deleted in lung cancer (28). In addition, a number of transcription factors (such as ZEB-1, p53, and ID-2) have been reported to regulate SEMA3F expression in lung, melanoma, and prostate cancer (29–31). Nevertheless, how SEMA3F is suppressed in breast cancer remains to be determined.

We have identified RORα as a transcriptional regulator of the SEMA3F gene. We show that breast cancer development and progression is associated with inactivation of the RORα-SEMA3F pathway. Restoring RORα expression in breast cancer cells suppresses their malignant and invasive phenotypes in 3D culture and in the xenograft model. Reducing SEMA3F expression in RORα-expressing cells partially rescued the malignant phenotypes. These findings reveal that the RORα suppresses breast tumor invasiveness by modulating cell microenvironment.

Materials and Methods

Antibodies and reagents

Edu staining kit and Alexa Fluor® 594 phalloidin were from Invitrogen. Matrigel (lrECM) and type I Collagen were from BD Bioscience. RORA and SEMA3F cDNA clones were purchased from (Open Biosystem). shRORA plasmids were purchased from Sigma. SMARTpool SEMA3F and non-targeting siRNA were purchased from Thermo Scientific. The following antibodies were obtained as indicated: RORα and Lamin A/C (Santa Cruz); tubulin, actin and α6 intergrin (Millipore), Flag (Sigam); Ki67 (Vector Laboratories). Phosphorylated Akt and Akt (cell signaling); phosphorylated MEK and MEK (Cell Signaling).

Cell Culture and virus preparation

HMT-3522 S1 and T4-2 cells (a kind gift from Dr. Mina J Bissell) were maintained on tissue culture plastic as previously described (17). MDA-MB 231 cells (ATCC) were propagated in DMEM/F12 (Sigma) with 10% fetal bovine serum (Invitrogen). 3D laminin-rich extracellular matrix (3D lrECM) on-top cultures (32) were prepared by trypsinization of cells from tissue culture plastic, seeding of single cells on top of a thin gel of Engelbreth-Holm-Swarm (EHS) tumor extract (Matrigel: BD Biosciences), and addition of medium containing 5% EHS. S1 cells were seeded at a density of 3.1×10^4 cells per cm^2; T4 and MDA-MB 231 cell lines were seeded at 2.1×10^4 and 1.4×10^4 cells per cm^2. S1 and T4-2 were maintained in their propagation medium with media change every two days. MDA-MB 231 cells were maintained in H14 medium with 1% fetal bovine serum.

Flag-tagged RORA cDNA and SEMA3F cDNA were cloned into pCDH1 plasmid and generated expression vector pCDH1-RORAl-Flag and pCDH1-SEMA3F-Flag. 293 FT cells were transfected with pCDH1 or shRNA vector (Sigma) plus packaging lentivector using lipofectamine (Invitrogen). Malignant and non-malignant HMECs were infected with lentivirus and selected by puromycin 48h after infection.

Invasion Assay and Migration Assay

The Transwells (Corning) were coated with 60 μl 1mg/ml Matrigel and incubated for 30 min at 37°C. HEMCs were plated in 200 μl on top of the Transwell filter and incubated in 37°C 5% CO2 for 24 h. The invaded cells on the bottom face of the filter were fixed by methanol and stained with 8% crystal violet.

Vector control or RORα-expression MDA-MB-231 cells (0.04×10^6) were placed on type I collagen pre-coated 35 mm dishes in DMEM/F12 medium containing 2% FBS and 4 ng/ml EGF. After 2 h incubation at 37°C, images were taken by live cell/incubator imaging system (Nikon Biostation IMQ) every 10 min for 8 h.

Luciferase Report Assay

A DNA fragment containing SEMA3F promoter region (from −1513 to −1240) was amplified from human genomic DNA using primers 5′-GCGGGTACCGCTGGAGATAGTGATAGAAGTGGC-3′ and 5′-GCGAAGCTTAGGTGAGCAAACACCATCCT-3′ then cloned into luciferase report vector pGL4. A deletion (RORA response region from −1372 to −1360) mutant was constructed by primers 5′-CACTCATCTCCCTGAGGTCACCACCACTG-3′ and 5 ′-ACCTCAGGGAGATGAGTGGGGATGAGGAG-3′. HEK 293 cells were transient transfected with pCDH1-RORA-Flag, pGL4-SEMA3F promoter and renilla luciferace vector. Cells lysate were collected for the luciferase assay 24 h after transfection.

Immunofluorescence and Immunohistochemistry

Cells in lrECM gel were smeared on slides, dried briefly, and fixed with 4% paraformaldehyde and permeabilized with 0.5 % Triton X-100. Immunostaining was performed as previous described (18). Stained samples were imaged using a Nikon upright epifluorescence microscope or a confocal system comprised of an Olympus IX81 microscope.

Tissue array (Biomax; Pantomics) and xenograft tumor sections were de-paraffined and hydrated from xylene, 100% estrodial, 95% estrodial, 85% estrodial and 70% estrodial to PBS solution. Endogeneous peroxidase was blocked by incubation with 3% H_2O_2 for 20 min. Antigen retrieval was done by steaming in citrate sodium buffer for 30 min. Slides were incubated with antibodies at 4°C overnight, then the sections were incubated with goat anti-rabbit IgG conjugated with horseradish peroxidase at room temperature for 60 min. The conjugated antibody was detected by diaminobenzidine (DAB), and images were taken by Nikon and scored blindly.

Western blot analysis and RT-PCR

Cells grown on plastic and filters were lysed *in situ* in RIPA buffer [1% Nonidet P-40, 0.5% deoxycholate, 0.2% SDS, 150 mM sodium chloride, 50 mM Tris·HCl (pH 7.4) containing phosphatase and protease inhibitor cocktails (Calbiochem)]. Cells in 3D lrECM were isolated as colonies by using ice-cold PBS plus 5 mM EDTA and thereafter lysed in RIPA buffer as described previously (21). Equal amounts of protein lysates were subjected to SDS gel electrophoresis, immunoblotted and detected with an ECL system (Pierce).

Total RNA was extracted from cells using Trizol reagent (Invitrogen). cDNA was synthesized using SuperScript First Strand Synthesis kit (Invitrogen) from 0.5–1.0 μg RNA samples. cDNA synthesis was performed with SuperScript III First-Strand Synthesis System according to the manufacturer's instructions. Quantitative RT-PCR reactions were carried out using SYBR Green PCR master mix reagents on an ABI 7500 Fast Real-Time PCR System (Applied Biosystems, USA). Thermal cycling was conducted at 95°C for 30 s, followed by 40 cycles of amplification at 95°C for 5 s, 55°C for 30 s and 72°C for 15 s. The relative quantification of gene expression for each sample was analyzed by the ΔCt method. The following primers were used to amplify SEMA3F: 5′-CTTTACTTCTTCTTCCGTGAGCG-3′ and 5′-GACAGCGTAAATGACAGGGTT-3′; 18S rRNA: 5′-ACCTGGTTGATCCTGCCAGT-3′ and 5′-CTGACCGGGTTGGTTTTGAT-3′.

Chromatin immunoprecipitation (ChIP) assay

The ChIP assay was performed based on the Upstate Biotechnology ChIP protocol with a few modifications (18, 33). After formaldehyde cross-linking, nuclei were isolated with a nuclei isolation kit (Sigma) and resuspended in ChIP lysis buffer (1% SDS, 10 mM EDTA, 50 mM Tris-HCl pH8.0) containing protease inhibitor cocktail. Protein-DNA complexes were immunoprecipitated as per the Upstate protocol. Isolated DNA was then analyzed by quantitative PCR using the following primers: 5′-TGGAAGGGATGGTGTTGGAAG-3′ and 5′-ACAGGCAGGGCATTTGAGGT-3′.

Xenograft experiment

Six-week-old female BalB/C null/null mice were randomly grouped and subcutaneously injected with 2×10^6 control or RORα-expression T4-2 cells (in PBS buffer, with 50% matrigel). The control or RORα-expression MDA-MB-231/Luc cells were injected into mammary fat pad at 2×10^6 cells/per gland of SCID mouse, and the tumor volume was measured using an in vivo imaging system (IVIS). All of the procedures during our study were performed within the guidelines of the Division of Laboratory Animal Resources at the

University of Kentucky. Tumors were measured with a caliper every three days for three weeks. After sacrificing all mice, the tumor samples were weighed, imaged, and fixed with 4% PFA for section.

Kaplan M eier survival analysis and other statistical analysis

We examined RORα expression in 404 breast tumor expression arrays taken from studies by Wang *et al*. (34) (n=286) and Chin *et al*. (35) (n=118). In each data set, the tumor samples were classified into RORα low (*si*≤(mean [*S*]-1/2×standard deviation [*S*])), RORα high (*si*≥(mean [*S*]+1/2×standard deviation [*S*])), and RORα medium based on the RORα mRNA level. This method allowed us to compare relative ROR*a* expression levels across both data sets fused as a single group of patients (36). The association between RORα expression and clinical pathologic parameters was evaluated using the Fisher's exact test. Significant differences in survival time were assessed using the Cox proportional hazard (log-rank) test. All reported *P* values were two-tailed. Association between RORα and SEMA3F was evaluated using the Fisher's exact test. Statistical analysis was performed using SigmaPlot (Systat Software, Inc) and SAS (version 9.2; SAS Institute Inc).

Results

Reduced RORα expression is associated with disruption of polarized acinar structure and breast cancer development

To determine which genes are associated with cell polarization and acinar morphogenesis in 3D culture, we analyzed expression profiles of non-malignant S1, malignant T4-2, and a variety of phenotypically reverted T4-2 cells (the cells are treated with a number of inhibitors targeted to EGFR, β1-integrin, or MMPs). Using Gene Set Enrichment Analyses (GSEA), we identified RORα as one of the transcription factors that induces gene expression in polarized S1 and reverted T4-2 cells (T4R) (Figure 1a). To determine whether RORα is differentially activated in polarized and disorganized HEMCs, we assessed RORα protein levels in S1, T4-2, and reverted T4-2 (T4R) cells in 3D culture. We found that both total and nuclear RORα levels were up-regulated in polarized S1 and reverted T4-2 cells compared to disorganized T4-2 cells (Figure 1b). This up-regulation correlates with activation of the potential RORα targeted genes. In addition, we performed reverse transcription polymerase chain reaction (RT-PCR) with isoform-specific primers to determine which RORα isoforms are expressed in HMECs. Only RORα1 and RORα4 transcripts were amplified from S1 and T4-2 cells (data not shown).

Breast cancer development is accompanied by disruption of tissue polarity; therefore we next determined whether RORα expression is repressed in breast cancer cell lines and tissues. We assessed the protein levels of RORα in 12 malignant and non-malignant HMECs cultured in 3D Matrigel. Results showed that protein expression of RORα was significantly reduced in breast cancer cells compared to non-malignant cells (Figure 1c). Immunohistochemistry (IHC) analysis of a panel of normal and malignant breast tissues also demonstrated that RORα protein expression was relatively downregulated in human breast cancer (Figure 1d, e). By analyzing mRNA levels of RORα in a published microarray dataset generated from more than 1000 human malignant and non-malignant breast tissues (37), we found that RORα transcription was significantly downregulated in cancer tissues (Supplemental Table 1). Together these results indicate that breast cancer development is accompanied by reduced RORα expression.

RORα inhibits cell invasion and suppresses aggressive phenotypes of breast cancer cells

To explore the functional relevance of down-regulation of RORα to malignant phenotypes of breast cancer cells, we restored RORα expression in T4-2 cells and examined their

morphologies in 3D culture. T4-2 cells were infected with lentivirus containing control or RORα-expressing vectors, and then expression of RORα was confirmed by western blot (Figure 2a). RORα-expressing T4-2 cells formed round spheroid structures in 3D culture, and colony formation size was significantly reduced compared to the control cells (Figure 2b and Supplemental Figure 1). Staining with α6-integrin (basal marker) and Ki67 antibodies revealed that RORα expression reprogrammed the cells to form polarized and growth-arrested structures (Figure 2b, c, d). It has been shown that activation of PI3K and MEK pathways disrupts the polarized acinar structures and cell invasion (38–40). Thus we assessed the activity of these two pathways by measuring the phosphorylation of Akt and MEK. We found that restoring RORα expression in T4-2 cells reduced the levels of phosphorylated Akt and MEK (Figure 2e), suggesting that PI3K-Akt and MEK pathways are involved in RORα-regulated cell polarization. Since cell polarization is often associated with reduced invasiveness, we examined the invasiveness of RORα-expressing cells in the Transwell assay. Results showed that expression of RORα1 or RORα4 significantly inhibited invasion of T4-2 cells (Figure 2f).

To investigate the effect of RORα on tumor growth *in vivo*, the control and RORα1-expressing T4-2 cells were subcutaneously injected into the flanks of female athymic nude mice. We found that tumor growth was delayed in the RORα1 group compared to the control group (Figure 2g), and that the tumors formed by RORα1-expressing cells were significantly smaller than the tumors formed by control cells (Figure 2h). Ki67 staining showed that the tumor cells in RORα1-expressing tumors were less proliferative than the cells in the control group (Figure 2i), which may cause the decrease of tumor volume in RORα-expressing tumors.

Restoring RORα expression in another breast cancer cell line, MDA-MB 231, also suppressed the aggressive phenotypes in 3D culture. For instance, the invasive branching structures and colony size were significantly reduced in RORα-expressing cells (Figure 3a, b); cell proliferation and invasion were also significantly inhibited by RORα (Figure 3c, d). By tracking single cell movement using live cell imaging, we also found that expression of RORα significantly inhibited cell migration in MDA-MB 231 cells (Figure 3e, f). Thus, reduction of invasive branching structures in RORα-expressing cells is most likely due to inhibition of cell migration and invasion. In addition, we have transplanted the control and RORα1-expressing MDA-MB 231 cells into the mammary gland fat pads of female SCID mice. We found that RORα1-expressing MDA-MB 231 cells formed much smaller tumor than control cells (Figure 3g, h).

Since disruption of acinar structure is accompanied by reduced RORα expression in 3D culture, we asked whether silencing RORα disturbs acinar morphogenesis in non-malignant HMECs. S1 cells were infected with lentivirus containing shRORα or control shRNA, and knockdown efficiency was assessed by western blot (Figure 4a). The cells with reduced RORα expression formed disorganized structures with a slight increase in colony size compared to the control S1 cells in 3D culture (Figure 4b, c). Staining of α6-integrin demonstrated that the number of polarized colonies is significantly decreased in the RORα knockdown cells (Figure 4d). These results indicate that RORα modulates polarization of HMECs, which is required for acinar morphogenesis.

SEMA3F is a RORα target gene and mediates its inhibitory activity on cell invasion

To understand how inactivation of RORα promotes breast tumor progression, we set out to identify RORα target genes mediating its suppressive activity in HMECs. SEMA3F, a secretary protein with tumor suppressor function (28), is one of the potential RORα target genes identified by GSEA analysis. It has been shown that SEMA3F produced by cancer cell acts in a paracrine and autocrine manner inhibiting cell migration and invasion (25–27).

By analyzing protein in the conditional medium, we found that the secretion of SEMA3F is significantly up-regulated in S1 and reverted T4 cells (T4R) compared to malignant T4-2 cells (Figure 5a), and restoring RORα expression in T4-2 cells enhanced the SEMA3F production (Figure 5b). The reduction of SEMA3F expression was also observed in breast cancer cell lines MDA-MB 231 and BT549 compared to non-malignant MCF10A cells (Supplemental Figure 2). To further verify whether SEMA3F is regulated by RORα at the transcription level, we measured the SEMA3F mRNA in RORα-expressing T4-2 and MDA-MB 231 cells. Quantitative RT-PCR results showed that SEMA3F transcription was induced by RORα in T4-2 and MDA-MB 231 cells (Figure 5c); while knockdown of RORα in non-malignant S1 cells significantly reduced SEMA3F transcription (Figure 5d).

By analyzing the genomic sequence of SEMA3F, we identified two potential RORα binding sites from the proximal promoter region of SEMA3F (−1372 to −1360, −663 to −652). To verify whether RORα directly binds to these two regions, we performed chromatin immunoprecipitation (ChIP) analysis. We found that binding of RORα to the −1372 to −1360 region was significantly enhanced in RORα-expressing T4-2 cells (Figure 5e), but little interaction was detected between RORα and the −663 to −652 region (data not shown). To assess whether RORα induces transcription of SEMA3F through this region, we amplified and cloned the SEMA3F promoter into pGL4 luciferase vector. The luciferase reporter construct was co-transfected with RORα expression vector into HEK293 cells. The activity of firefly/renella luciferase showed that expression of RORα1 drastically induced transcription driven by SEMA3F promoter (Figure 5f). To further verify whether the binding of RORα to this site is functionally important, the sequence from −1372 to −1360 was deleted in the SEMA3F promoter and cloned into the luciferase reporter construct. We found that deletion of the RORα binding site in the SEMA3F promoter significantly reduced the transcription activity (Figure 5g), indicating that binding of RORα to this region is critical for the transcriptional activation of SEMA3F.

To determine whether RORα-induced SEMA3F is functionally relevant to the suppressive activity of RORα in cancer cells, we silenced SEMA3F expression in RORα-expressing cancer cells using siRNA (Figure 6a). We found that knockdown of SEMA3F in RORα-expressing MDA-MB 231 cells rescued the invasive branch structure in 3D culture (Figure 6b, c). Moreover, silencing SEMA3F expression significantly enhanced cell invasion in RORα-expressing MDA-MB 231 and T4-2 cells. (Figure 6d). Next, we examined the activation of PI3K-Akt and MEK pathway in those cells. We found that downregulated of SEMA3F enhanced phosphorylation of MEK, but had little effects on Akt phosphorylation (Figure 6e). Since activation of MEK pathway has been shown to promote cancer invasion in culture and *in vivo* (40, 41), these results suggest that the RORα-SEMA3F axis suppresses invasion of cancer cells through inhibiting MEK pathway. Moreover, RORα-expressing MDA-MB 231 cells tended to invade in surrounding tissue in SCID mice after SEMA3F was silenced, but knockdown of SEMA3F had little effect on tumor growth (Figure 6f, g). We also expressed SEMA3F in T4-2 and MDA-MB 231 cells. We found that the majority of SEMA3F-expressing cancer cells formed non-invasive structures in 3D culture (Supplemental Figure 3). These results suggest that the tumor suppressor function of RORα is at least partially conferred by SEMA3F.

Reduced expression of RORα and SEMA3F is associated with poor prognosis

To address the clinical relevance of a functional link between RORα and SEMA3F, we examined protein and mRNA expression of RORα and SEAM3F in cohorts of human breast cancers. IHC analysis of a panel of 259 breast cancer tissues revealed that the nuclear levels of RORα significantly correlated to protein expression of SEMA3F (Figure 7a and Table 1). Moreover, high grading tumors contains more RORα and SEMA3F double negative samples compared to low grading tumors (Figure 7b and Supplemental Table 2), suggesting that

inactivation of RORα and SEMA3F is associated with breast cancer progression. To further determine whether reduced RORα or SEMA3F expression is associated with prognosis of patients, we assessed the association between mRNA levels of these two genes and patient survival using the published microarray data generated from more than 400 breast cancer tissue samples (34, 35). Breast cancer patients were divided into three groups based on RORα or SEMA3F mRNA levels (low, moderate and high). Kaplan-Meier log rank analysis showed that patients whose tumor had low RORα or SEMA3F expression levels had a significantly shorter survival period (Figure 7c, d), suggesting that inactivation of the RORα-SEMA3F pathway correlates with poor clinical outcome.

Discussion

Disruption of acinar structures during breast cancer development is accompanied by two types of microenvironmental changes (42): 1) inhibiting suppressive microenvironmental signals, such as proper cell-cell and cell-basement membrane adhesion, MMP inhibitors, and suppressive microenvironmental factors (43); 2) enhancing the promotional microenvironmental cues, including various growth factors and cytokines, ECM degradation enzymes and activation of angiogenesis, which has been extensively studied and used as therapeutic target in clinical trials. By analyzing the global expression profiles of polarized and disorganized HMECs in 3D culture, we have identified a number of microenvironment-related genes down-regulated in disorganized cells, including tumor suppressor SEMA3F. We show that RORα is a transcriptional regulator of SEMA3F and is repressed during breast cancer development and progression. Restoring RORα or SEMA3F expression in breast cancer cells inhibits aggressive phenotypes in 3D culture and tumor growth *in vivo*. We conclude that the RORα-SEMA3F axis provides a suppressive microenvironment in normal tissue, inactivation of which promotes breast cancer development and progression.

Loss of polarity is an important morphological event in breast cancer development, which is accompanied by extensive changes in global gene expression profiles (37, 44). By searching for over-represented motifs in the promoter regions of the differentially expressed genes between polarized and disorganized cells, we showed that RORα induces gene expression in polarized HMEC cells. We also demonstrate that expression of RORα protein is significantly reduced in breast cancer cell lines and cancer tissues, and this reduction is associated with disruption of the acinar structure in 3D culture and cancer progression *in vivo*. Silencing RORα expression in non-malignant S1 cells disrupts the polarized acinar morphogenesis, suggesting that RORα is involved in normal mammary gland development. We also showed that restoring RORα expression in breast cancer cells significantly inhibits tumor growth in nude mice and suppressed malignant phenotypes in 3D culture. Furthermore, patients with reduced expression of RORα in cancer tissue have significantly shorter survival. Together these results indicate that inactivation of RORα promotes breast cancer development and progression by enhancing cell invasion and disturbing normal tissue architecture.

Microarray analysis has shown that RORα mRNA levels are down-regulated in many types of cancer, including breast, lung, and colon (45). Because the RORα gene locates at a common fragile site that is often deleted in cancer, it was proposed that inactivation or downregulation of RORα in cancer cells is caused by genomic instability. However, in the HMT-3522 breast cancer progression series, we showed that downregulation of RORα in cancer cells was reversible, suggesting that RORα is not regulated at the genomic level in those cell lines. We also analyzed the published microarray and CGH data generated from a panel of breast cancer cell lines (35) and did not find a correlation between RORα mRNA levels and gene copy numbers (data not shown). We showed that blocking the EGFR pathway with tryphostin significantly increased protein levels of RORα and mRNA levels of

RORα target gene in T4-2 cells, while RORα mRNA level has little change upon inhibition of those pathways (data not shown). Therefore, it is most likely that RORα is regulated at the protein level in HMT-3522 cell lines.

RORα has been considered a constitutively activated nuclear receptor, but a number of pathways are involved in post-translational regulation of its activity. For instance, RORα can be phosphorylated by ERK and PKC in neuron and HeLa cells. Both ERK- and PKC-dependent phosphorylation suppresses the transcription activity of RORα (46, 47). In addition, the RORα protein is rapidly turned over in Cos-1 cells, and the protein level increases upon inhibition of the 26S proteasome complexes (48), indicating that the Ub-proteasome pathway is involved in degradation of RORα protein. A recent study sheds light on the roles of post-translational modification of RORα in colon cancer development (6). Lee *et al.* showed that Wnt5a/PKCa induces phosphorylation on serine residue 35 of RORα. The phosphorylated RORα attenuates the Wnt signaling pathway through binding to β-catenin at Wnt3a-activatable promoters to suppress the transcription of Wnt/β-catenin target genes (6). Our results showed that deletion of the ligand-binding or DNA-binding domains in RORα drastically reduced the inhibitory activity of RORα (data not shown), thus we proposed that transcription activity of RORα is required for the tumor suppressor function in breast cancer.

SEMA3F is one of the suppressive microenvironmental factors often inactivated in metastatic cancer and the inactivation has been attributed to gene deletion in lung cancer (28). Reduced mRNA levels of SEMA3F are associated with poor clinical outcome in breast cancer patients (Figure 7d), thus loss of SEMA3F function may contribute to breast cancer progression. We found that expression and secretion of SEMA3F are downregulated in disorganized HMECs compared to polarized cell in 3D culture, parallel to RORα inactivation. Using ChIP and luciferase reporter assays, we proved that SEMA3F is a RORα target gene. Although the tumor suppressor function of SEMA3F has been largely attributed to its anti-angiogenesis activity, we showed that introducing SEMA3F in breast cancer cells suppressed the aggressive phenotypes in 3D culture, and knockdown of SEMA3F in RORα-expression cancer cells rescued cell invasiveness, suggesting that SEMA3F also targets breast cancer cells. In fact, SEMA3F receptor NRPs have been detected in breast cancer cells (49), and it has been shown that expression of SEMA3F in breast cancer cells inhibits cell migration and invasion (50). Mammary specific knockout of NRP2 impairs branch morphogenesis and ductal outgrowth in mouse mammary gland, suggesting that NRP2 is crucial for cell migration and invasion (51). We show that SEMA3F receptor nerophilin 2 (NRP2) are expressed in a number of breast cell lines, including T4-2 and MDA-MB 231 cells (Supplemental Figure 4). Moreover, NRPs have been identified as co-receptors of integrin and VEGFR. Thus, SEMA3F may suppress breast cancer invasion and MEK phosphorylation by disturbing the interaction between NRPs and other receptors.

However, silencing SEMA3F in RORα-expressing cancer cells has little effect on tumor growth, suggesting that the tumor suppressor function of RORα involves other target genes and pathways. We have identified multiple potential RORα targets genes from the GSEA analysis, such as FBXW7 and ANGPT1, which have been shown to inhibit cell proliferation and cancer progression (52–54). In myoblast cell line C2C12, RORα induces activation of the cdk-inhibitor p21 waF1/cipl, a marker for cell cycle exit (55). Wnt/β-Catenin pathway has been linked to various types of cancers, including breast. Since RORα has been identified as an inhibitor of the Wnt signal, RORα may suppresses breast tumor growth by inhibiting Wnt target genes. In addition, RORα negatively interferes with the NF-κB signaling pathway and suppresses inflammatory response by inducing IκBα (56). These RORα target genes and pathways may also mediate inhibitory activities of RORα in breast cancer cells. Moreover, RORα has been identified as a transcriptional regulator of aromatase

in MCF7 and T47D (57) and as a potential ERα partner (58), suggesting that RORα may have different target genes and functions in ER positive cells. Therefore, it is important to address functional linkage between RORα and its target genes in different subtypes of breast cancer in the future.

In summary, our findings reveal that RORα is crucial for maintenance of a suppressive microenvironment in normal mammary tissue, and inactivation of RORα in breast cancer cells promotes cancer invasion by reducing SEMA3F expression. Thus, understanding how RORα is inactivated in breast cancer and identifying its ligands or agonists may lead to the discovery of a novel therapeutic strategy for the treatment of breast cancer.

Supplementary Material

Refer to Web version on PubMed Central for supplementary material.

Acknowledgments

R.X. is deeply grateful to Dr. Mina J. Bissell (Lawrence Berkeley National Laboratory) for her training and support. We appreciate the advice from Dr. Rouzan Karabakhtsian on IHC and H&E staining and analysis. We thank Dr. Nathan L. Vanderford for scientific editing and Dr. Piotr Rychahou for the assistance in the animal experiments. This work was supported by grants from NCI (P30 CA147886 to B.M.E), ACS (IRG 85-001-22 to R.X), AHA (12SDG8600000 to R.X.).

References

1. Jetten AM. Retinoid-related orphan receptors (RORs): critical roles in development, immunity, circadian rhythm, and cellular metabolism. Nucl Recept Signal. 2009; 7:e003. [PubMed: 19381306]
2. Jetten AM, Kurebayashi S, Ueda E. The ROR nuclear orphan receptor subfamily: critical regulators of multiple biological processes. Prog Nucleic Acid Res Mol Biol. 2001; 69:205–47. [PubMed: 11550795]
3. Carlberg C, Hooft van Huijsduijnen R, Staple JK, DeLamarter JF, Becker-Andre M. RZRs, a new family of retinoid-related orphan receptors that function as both monomers and homodimers. Mol Endocrinol. 1994; 8:757–70. [PubMed: 7935491]
4. Dussault I, Fawcett D, Matthyssen A, Bader JA, Giguere V. Orphan nuclear receptor ROR alpha-deficient mice display the cerebellar defects of staggerer. Mech Dev. 1998; 70:147–53. [PubMed: 9510031]
5. Matysiak-Scholze U, Nehls M. The structural integrity of ROR alpha isoforms is mutated in staggerer mice: cerebellar coexpression of ROR alpha1 and ROR alpha4. Genomics. 1997; 43:78–84. [PubMed: 9226375]
6. Lee JM, Kim IS, Kim H, Lee JS, Kim K, Yim HY, et al. RORalpha attenuates Wnt/beta-catenin signaling by PKCalpha-dependent phosphorylation in colon cancer. Mol Cell. 2010; 37:183–95. [PubMed: 20122401]
7. Steinmayr M, Andre E, Conquet F, Rondi-Reig L, Delhaye-Bouchaud N, Auclair N, et al. staggerer phenotype in retinoid-related orphan receptor alpha-deficient mice. Proc Natl Acad Sci U S A. 1998; 95:3960–5. [PubMed: 9520475]
8. Dzhagalov I, Giguere V, He YW. Lymphocyte development and function in the absence of retinoic acid-related orphan receptor alpha. J Immunol. 2004; 173:2952–9. [PubMed: 15322153]
9. Sato TK, Panda S, Miraglia LJ, Reyes TM, Rudic RD, McNamara P, et al. A functional genomics strategy reveals Rora as a component of the mammalian circadian clock. Neuron. 2004; 43:527–37. [PubMed: 15312651]
10. Lau P, Nixon SJ, Parton RG, Muscat GE. RORalpha regulates the expression of genes involved in lipid homeostasis in skeletal muscle cells: caveolin-3 and CPT-1 are direct targets of ROR. J Biol Chem. 2004; 279:36828–40. [PubMed: 15199055]
11. Zhu Y, McAvoy S, Kuhn R, Smith DI. RORA, a large common fragile site gene, is involved in cellular stress response. Oncogene. 2006; 25:2901–8. [PubMed: 16462772]

12. Xu R, Mao JH. Gene transcriptional networks integrate microenvironmental signals in human breast cancer. Integr Biol (Camb). 2011; 3:368–74. [PubMed: 21165486]
13. Bissell MJ, Weaver VM, Lelievre SA, Wang F, Petersen OW, Schmeichel KL. Tissue structure, nuclear organization, and gene expression in normal and malignant breast. Cancer Res. 1999; 59:1757–63s. discussion 63s–64s. [PubMed: 10197593]
14. Bissell MJ, Radisky D. Putting tumours in context. Nat Rev Cancer. 2001; 1:46–54. [PubMed: 11900251]
15. Sgroi DC. Preinvasive breast cancer. Annu Rev Pathol. 2010; 5:193–221. [PubMed: 19824828]
16. Zhang C, Yu D. Microenvironment determinants of brain metastasis. Cell Biosci. 2011; 1:8. [PubMed: 21711688]
17. Petersen OW, Ronnov-Jessen L, Howlett AR, Bissell MJ. Interaction with basement membrane serves to rapidly distinguish growth and differentiation pattern of normal and malignant human breast epithelial cells. Proc Natl Acad Sci U S A. 1992; 89:9064–8. [PubMed: 1384042]
18. Xu R, Nelson CM, Muschler JL, Veiseh M, Vonderhaar BK, Bissell MJ. Sustained activation of STAT5 is essential for chromatin remodeling and maintenance of mammary-specific function. J Cell Biol. 2009; 184:57–66. [PubMed: 19139262]
19. Barcellos-Hoff MH, Aggeler J, Ram TG, Bissell MJ. Functional differentiation and alveolar morphogenesis of primary mammary cultures on reconstituted basement membrane. Development. 1989; 105:223–35. [PubMed: 2806122]
20. Weaver VM, Petersen OW, Wang F, Larabell CA, Briand P, Damsky C, et al. Reversion of the malignant phenotype of human breast cells in three-dimensional culture and in vivo by integrin blocking antibodies. J Cell Biol. 1997; 137:231–45. [PubMed: 9105051]
21. Wang F, Weaver VM, Petersen OW, Larabell CA, Dedhar S, Briand P, et al. Reciprocal interactions between beta1-integrin and epidermal growth factor receptor in three-dimensional basement membrane breast cultures: a different perspective in epithelial biology. Proc Natl Acad Sci U S A. 1998; 95:14821–6. [PubMed: 9843973]
22. Liu H, Radisky DC, Nelson CM, Zhang H, Fata JE, Roth RA, et al. Mechanism of Akt1 inhibition of breast cancer cell invasion reveals a protumorigenic role for TSC2. Proc Natl Acad Sci U S A. 2006; 103:4134–9. [PubMed: 16537497]
23. Yamauchi K, Mizushima S, Tamada A, Yamamoto N, Takashima S, Murakami F. FGF8 signaling regulates growth of midbrain dopaminergic axons by inducing semaphorin 3F. J Neurosci. 2009; 29:4044–55. [PubMed: 19339600]
24. Gammill LS, Gonzalez C, Gu C, Bronner-Fraser M. Guidance of trunk neural crest migration requires neuropilin 2/semaphorin 3F signaling. Development. 2006; 133:99–106. [PubMed: 16319111]
25. Shimizu A, Mammoto A, Italiano JE Jr. Pravda E, Dudley AC, Ingber DE, et al. ABL2/ARG tyrosine kinase mediates SEMA3F-induced RhoA inactivation and cytoskeleton collapse in human glioma cells. J Biol Chem. 2008; 283:27230–8. [PubMed: 18660502]
26. Potiron VA, Sharma G, Nasarre P, Clarhaut JA, Augustin HG, Gemmill RM, et al. Semaphorin SEMA3F affects multiple signaling pathways in lung cancer cells. Cancer Res. 2007; 67:8708–15. [PubMed: 17875711]
27. Bielenberg DR, Hida Y, Shimizu A, Kaipainen A, Kreuter M, Kim CC, et al. Semaphorin 3F, a chemorepulsant for endothelial cells, induces a poorly vascularized, encapsulated, nonmetastatic tumor phenotype. J Clin Invest. 2004; 114:1260–71. [PubMed: 15520858]
28. Xiang RH, Hensel CH, Garcia DK, Carlson HC, Kok K, Daly MC, et al. Isolation of the human semaphorin III/F gene (SEMA3F) at chromosome 3p21, a region deleted in lung cancer. Genomics. 1996; 32:39–48. [PubMed: 8786119]
29. Coma S, Amin DN, Shimizu A, Lasorella A, Iavarone A, Klagsbrun M. Id2 promotes tumor cell migration and invasion through transcriptional repression of semaphorin 3F. Cancer Res. 2010; 70:3823–32. [PubMed: 20388805]
30. Futamura M, Kamino H, Miyamoto Y, Kitamura N, Nakamura Y, Ohnishi S, et al. Possible role of semaphorin 3F, a candidate tumor suppressor gene at 3p21.3, in p53-regulated tumor angiogenesis suppression. Cancer Res. 2007; 67:1451–60. [PubMed: 17308083]

31. Clarhaut J, Gemmill RM, Potiron VA, Ait-Si-Ali S, Imbert J, Drabkin HA, et al. ZEB-1, a repressor of the semaphorin 3F tumor suppressor gene in lung cancer cells. Neoplasia. 2009; 11:157–66. [PubMed: 19177200]
32. Lee GY, Kenny PA, Lee EH, Bissell MJ. Three-dimensional culture models of normal and malignant breast epithelial cells. Nat Methods. 2007; 4:359–65. [PubMed: 17396127]
33. Xu R, Spencer VA, Bissell MJ. Extracellular matrix-regulated gene expression requires cooperation of SWI/SNF and transcription factors. J Biol Chem. 2007; 282:14992–9. [PubMed: 17387179]
34. Wang Y, Klijn JG, Zhang Y, Sieuwerts AM, Look MP, Yang F, et al. Gene-expression profiles to predict distant metastasis of lymph-node-negative primary breast cancer. Lancet. 2005; 365:671–9. [PubMed: 15721472]
35. Chin K, DeVries S, Fridlyand J, Spellman PT, Roydasgupta R, Kuo WL, et al. Genomic and transcriptional aberrations linked to breast cancer pathophysiologies. Cancer Cell. 2006; 10:529–41. [PubMed: 17157792]
36. Climent J, Perez-Losada J, Quigley DA, Kim IJ, Delrosario R, Jen KY, et al. Deletion of the PER3 gene on chromosome 1p36 in recurrent ER-positive breast cancer. J Clin Oncol. 2010; 28:3770–8. [PubMed: 20625127]
37. Ma XJ, Dahiya S, Richardson E, Erlander M, Sgroi DC. Gene expression profiling of the tumor microenvironment during breast cancer progression. Breast Cancer Res. 2009; 11:R7. [PubMed: 19187537]
38. Liu H, Radisky DC, Wang F, Bissell MJ. Polarity and proliferation are controlled by distinct signaling pathways downstream of PI3-kinase in breast epithelial tumor cells. J Cell Biol. 2004; 164:603–12. [PubMed: 14769856]
39. Beliveau A, Mott JD, Lo A, Chen EI, Koller AA, Yaswen P, et al. Raf-induced MMP9 disrupts tissue architecture of human breast cells in three-dimensional culture and is necessary for tumor growth in vivo. Genes Dev. 2010; 24:2800–11. [PubMed: 21159820]
40. Shin I, Kim S, Song H, Kim HR, Moon A. H-Ras-specific activation of Rac-MKK3/6-p38 pathway: its critical role in invasion and migration of breast epithelial cells. J Biol Chem. 2005; 280:14675–83. [PubMed: 15677464]
41. Pinkas J, Leder P. MEK1 signaling mediates transformation and metastasis of EpH4 mammary epithelial cells independent of an epithelial to mesenchymal transition. Cancer Res. 2002; 62:4781–90. [PubMed: 12183438]
42. Bissell MJ, Hines WC. Why don't we get more cancer? A proposed role of the microenvironment in restraining cancer progression. Nat Med. 2011; 17:320–9. [PubMed: 21383745]
43. Furuta S, Jeng YM, Zhou L, Huang L, Kuhn I, Bissell MJ, et al. IL-25 Causes Apoptosis of IL-25R-Expressing Breast Cancer Cells Without Toxicity to Nonmalignant Cells. Sci Transl Med. 2011; 3:78ra31.
44. Rizki A, Weaver VM, Lee SY, Rozenberg GI, Chin K, Myers CA, et al. A human breast cell model of preinvasive to invasive transition. Cancer Res. 2008; 68:1378–87. [PubMed: 18316601]
45. Lu Y, Yi Y, Liu P, Wen W, James M, Wang D, et al. Common human cancer genes discovered by integrated gene-expression analysis. PLoS One. 2007; 2:e1149. [PubMed: 17989776]
46. Duplus E, Gras C, Soubeyre V, Vodjdani G, Lemaigre-Dubreuil Y, Brugg B. Phosphorylation and transcriptional activity regulation of retinoid-related orphan receptor alpha 1 by protein kinases C. J Neurochem. 2008; 104:1321–32. [PubMed: 18005000]
47. Lechtken A, Hornig M, Werz O, Corvey N, Zundorf I, Dingermann T, et al. Extracellular signal-regulated kinase-2 phosphorylates RORalpha4 in vitro. Biochem Biophys Res Commun. 2007; 358:890–6. [PubMed: 17512500]
48. Moraitis AN, Giguere V. The co-repressor hairless protects RORalpha orphan nuclear receptor from proteasome-mediated degradation. J Biol Chem. 2003; 278:52511–8. [PubMed: 14570920]
49. Yasuoka H, Kodama R, Tsujimoto M, Yoshidome K, Akamatsu H, Nakahara M, et al. Neuropilin-2 expression in breast cancer: correlation with lymph node metastasis, poor prognosis, and regulation of CXCR4 expression. BMC Cancer. 2009; 9:220. [PubMed: 19580679]

50. Kigel B, Varshavsky A, Kessler O, Neufeld G. Successful inhibition of tumor development by specific class-3 semaphorins is associated with expression of appropriate semaphorin receptors by tumor cells. PLoS One. 2008; 3:e3287. [PubMed: 18818766]
51. Goel HL, Bae D, Pursell B, Gouvin LM, Lu S, Mercurio AM. Neuropilin-2 promotes branching morphogenesis in the mouse mammary gland. Development. 2011; 138:2969–76. [PubMed: 21693513]
52. Akhoondi S, Sun D, von der Lehr N, Apostolidou S, Klotz K, Maljukova A, et al. FBXW7/hCDC4 is a general tumor suppressor in human cancer. Cancer Res. 2007; 67:9006–12. [PubMed: 17909001]
53. Mao JH, Kim IJ, Wu D, Climent J, Kang HC, DelRosario R, et al. FBXW7 targets mTOR for degradation and cooperates with PTEN in tumor suppression. Science. 2008; 321:1499–502. [PubMed: 18787170]
54. Stoeltzing O, Ahmad SA, Liu W, McCarty MF, Wey JS, Parikh AA, et al. Angiopoietin-1 inhibits vascular permeability, angiogenesis, and growth of hepatic colon cancer tumors. Cancer Res. 2003; 63:3370–7. [PubMed: 12810673]
55. Burke L, Downes M, Carozzi A, Giguere V, Muscat GE. Transcriptional repression by the orphan steroid receptor RVR/Rev-erb beta is dependent on the signature motif and helix 5 in the E region: functional evidence for a biological role of RVR in myogenesis. Nucleic Acids Res. 1996; 24:3481–9. [PubMed: 8836172]
56. Delerive P, Monte D, Dubois G, Trottein F, Fruchart-Najib J, Mariani J, et al. The orphan nuclear receptor ROR alpha is a negative regulator of the inflammatory response. EMBO Rep. 2001; 2:42–8. [PubMed: 11252722]
57. Odawara H, Iwasaki T, Horiguchi J, Rokutanda N, Hirooka K, Miyazaki W, et al. Activation of aromatase expression by retinoic acid receptor-related orphan receptor (ROR) alpha in breast cancer cells: identification of a novel ROR response element. J Biol Chem. 2009; 284:17711–9. [PubMed: 19439415]
58. Gu F, Hsu HK, Hsu PY, Wu J, Ma Y, Parvin J, et al. Inference of hierarchical regulatory network of estrogen-dependent breast cancer through ChIP-based data. BMC Syst Biol. 2010; 4:170. [PubMed: 21167036]

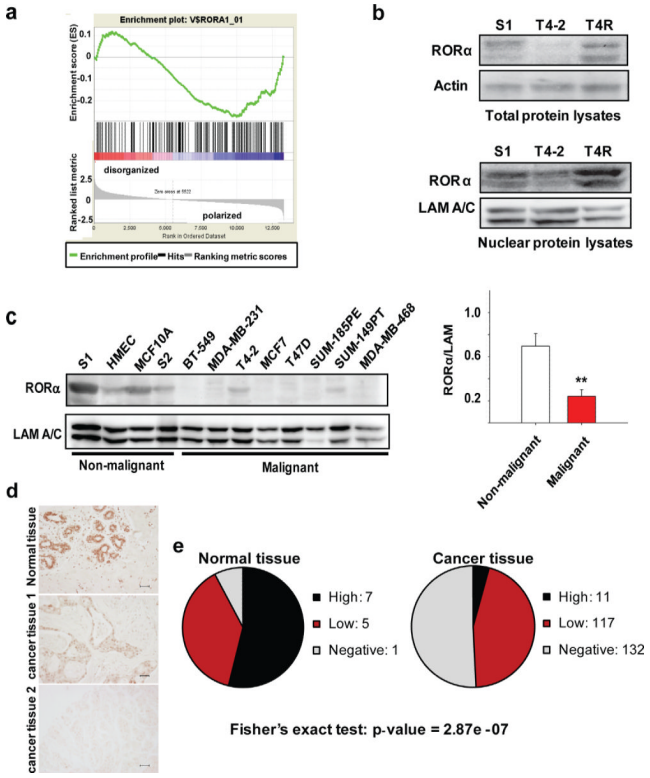

Fig 1.

Expression of RORα is down-regulated in breast cancer. (a) GSEA analysis identified RORα as a potential regulator of the genes whose expression are significantly up-regulated in polarized S1 and reverted T4-2 cells compared to disorganized T4-2 cells. (b) Total and nuclear protein levels of RORα were examined by immunoblotting in T4-2 cells, S1 and reverted T4-2 (T4R) cells. RORα level was down-regulated in disorganized T4-2 cells compared with polarized S1 cells and reverted T4-2 cells. (c) RORα expression was examined by immunoblotting in malignant (8) and nonmalignant (4) HMECs cultured in 3D Matrigel. RORα expression in malignant human breast cancer cells was significantly reduced compared to non-malignant human HMECs. The immunoblotting results were quantified by AlphaInnotech HD software. (d) Immunohistochemistry analysis of RORα expression in normal and malignant human breast tissue. Bar: 40 μm. (e) The pie graph showed staining intensity of RORα in normal breast tissue (n=13) and breast cancer tissue (n=260). The staining intensity was graded to three different levels. Most of normal breast tissue presented positive signal of RORα in nuclear of epithelial cells. In breast cancer tissue, most breast cancer tissue displayed weak positive signal of RORα (Low) and negative signal (Negative). Fisher's exact test showed that RORα protein level was significantly downregulated in breast cancer tissue compared to normal tissue.

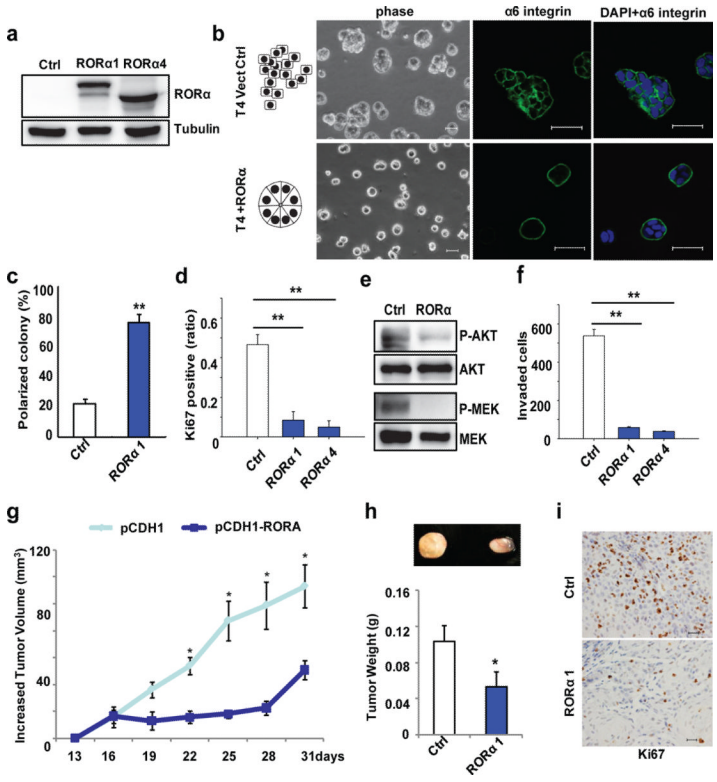

Fig 2.

Restoring RORα expression in malignant T4-2 cells suppressed the aggressive phenotypes in 3D culture and inhibited tumor growth *in vivo*. (a) RORα expression in infected cells was verified by western blot. (b) Phase and immunofluorescence images of RORα1-expressing and control T4-2 cells in 3D culture. RORα-expressing T4-2 cells formed polarized spheroids, whereas control T4-2 cells still maintained disorganized grape-like structures. Bar, 40μm. (c) Bar graph showing the ratio of polarized colony of the control and RORα-expressing T4-2 cells in 3D culture, n=3. (d) Ki67 staining analyzing proliferation of control and RORα1 expression T4-2 cells in 3D culture. RORα1 and RORα4 both inhibited proliferation of T4-2 cell. (e) Activation of Akt and MEK were assessed by western blot. Levels of phosphorylated Akt and MEK were both reduced in RORα-expressing T4-2 cells. (f) Transwell assay analyzing the invasion activities of control and RORα-expressing T4-2 cells, n=4. RORα expression significantly reduced cells invasion. (g) Growth Curve of tumors formed by RORα1-expressing and control T4-2 in nude mice, n=5. (h) Weight of tumors formed by RORα1- expressing and control T4-2 cells, n=5. (i) Ki67 IHC analysis of cell proliferation in tumor tissue. Cell proliferation in control tumor was much higher than that in RORα-expressing tumor. Bar: 20μm. * $p<0.05$, ** $p<0.01$.

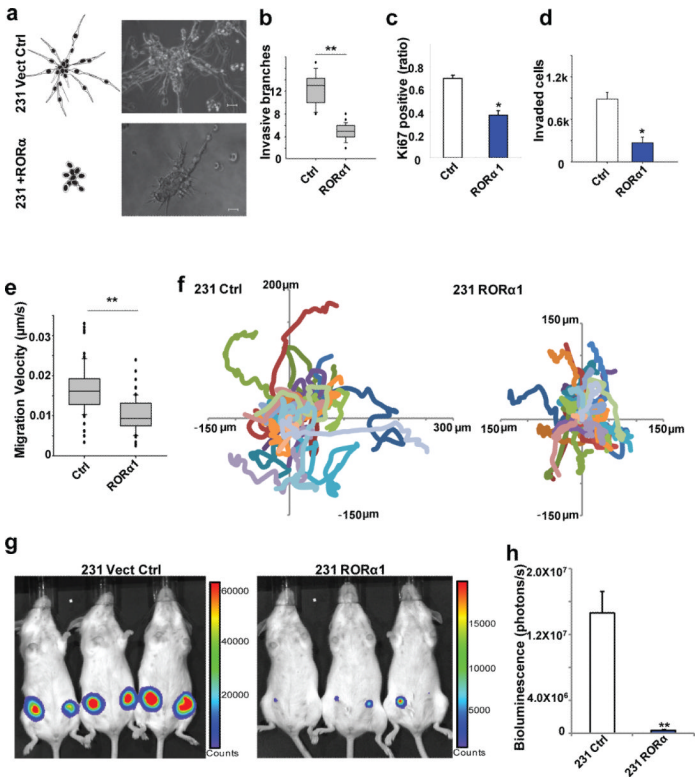

Fig 3.

RORα inhibited invasion and migration of MDA-MB-231 cells. (a) Phase images of MDA-MB-231 cells in 3D culture. Bar: 40 μm. (b) Bar graph of the invaded branches in MDA-MB-231 cells in 3D culture, n=22. (c) Ki67 staining analysis of cell proliferation in MDA-MB-231 cells. Proliferation of RORα1-expressing MDA-MB-231 cells was significantly inhibited compared with control cells. (d) Invasion analysis of control and RORα1-expressing MDA-MB-231 cells. RORα expression significantly inhibited cell invasion in MDA-MB 231 cells compared, n=4. (e) Single cell migration analysis of MDA-MB 231 cells. Migration of the RORα1-expressing cells was significantly reduced compared to the control cells, n=72. (f) The paths of cell migration in control and RORα-expressing MDA-MB 231 cells, n=25. (g) Growth of tumors formed by RORα1-expressing and control MDA-MB 231/Luc cells in SCID mice was imaged by IVIS (n=6). (h) Bar graph showing that tumor volume formed by RORα1-expressing cells was significantly reduced compared with control MDA-MB 231/Luc cells. * $p<0.05$, ** $p<0.01$.

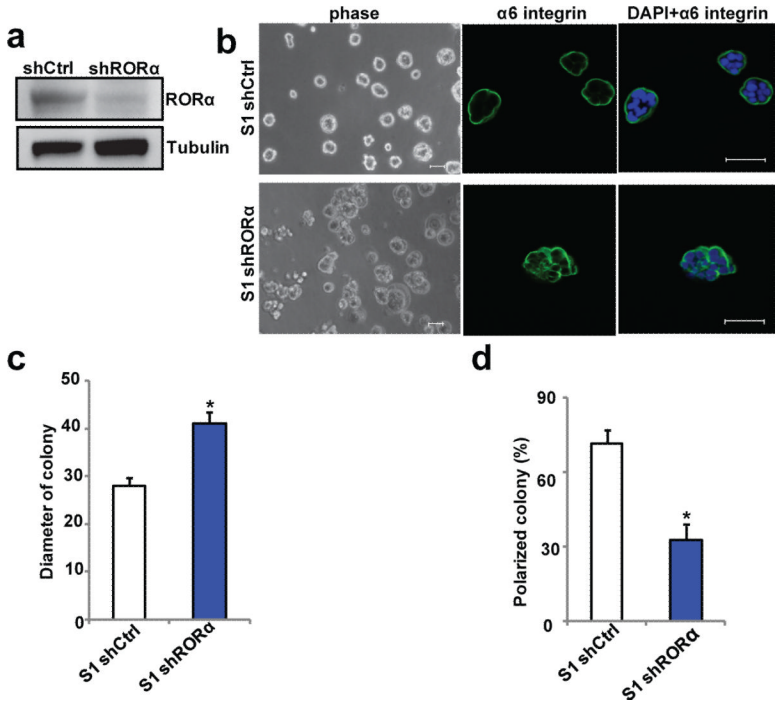

Fig 4.

Silencing RORα expression in nonmalignant S1 cells disrupts polarized acinar structures. (a) Immunoblotting analysis of knockdown efficiency of shRNA in S1 cells. (b) Phase and immunofluorescence images of S1 cells in 3D culture. Staining with α6 integrin antibody showed that RORα knockdown S1 cells formed disorganized structures in 3D culture. (c) Quantification of colony size of control and RORα knockdown S1 cells in 3D culture by measuring the diameter of 50 colonies. Knockdown RORα in S1 cells slightly increased the colony size. (d) Bar graph quantifying the ratio of polarized colonies of control cells and RORα knockdown S1 cells in 3D culture, n=3. Bar: 40μm. * $p<0.05$, ** $p<0.01$.

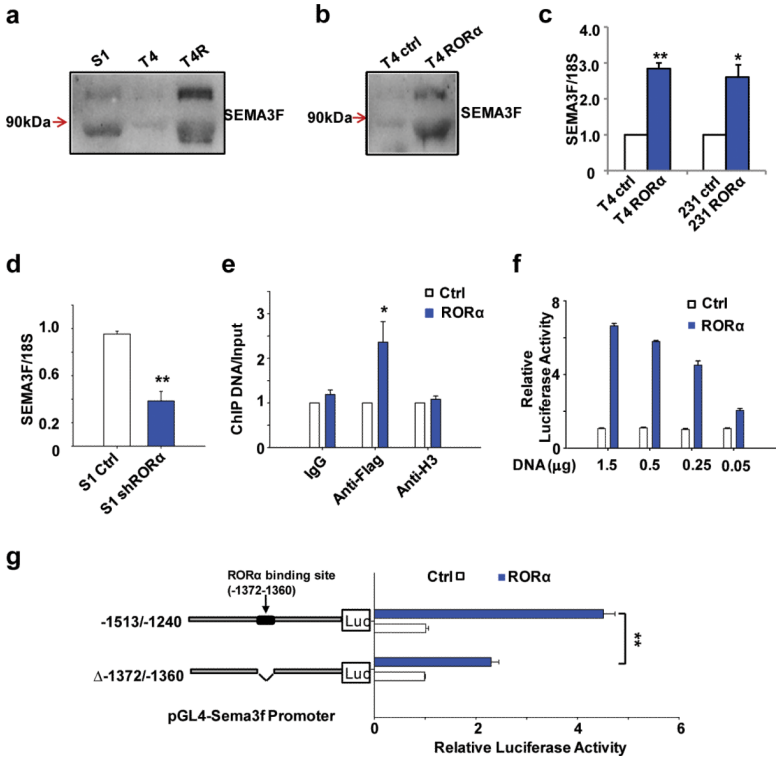

Fig 5.

SEMA3F is a RORα target gene mediating its tumor suppressor function. (a, b) SEMA3F secretion was assessed by western blot in the conditional medium of S1, T4-2, reverted T4-2 cells (T4R), and RORα-expressing T4-2 cells. Conditional medium isolated from same amount of cells was loaded, and SEMA3F levels were elevated in the medium of S1, reverted T4-2, and RORα-expressing T4-2 cells. (c) Quantitative RT-PCR measuring SEMA3F mRNA level in T4-2, reverted T4-2, and RORα-expressing T4-2 cells (n=4). (d) Quantitative RT-PCR measuring SEMA3F mRNA level in S1 and RORα knockdown S1 cells (n=6). (e) ChIP analyzing protein enrichment in the SEMA3F promoter region in control and RORα-expressing T4-2 cells. Binding of RORα protein but not histone H3 to SEMA3F promoter was significantly enhanced in RORα-expressing T4-2 cells, n=3. (f) Luciferase assay measuring the transcriptional activity of SEMA3F promoter (from residues −1513 to −1240) in response to RORα expression. RORα1 enhanced promoter activity of SEMA3F in a dose-dependent manner, n=4. (g) A deletion of RORE in SEMA3F promoter (from residues −1372 to −1360) was made and cloned into pGL4 vector. Promoter activity of SEMA3F in response to RORα was reduced by deletion of the RORE, n=4. * $p<0.05$, ** $p<0.01$.

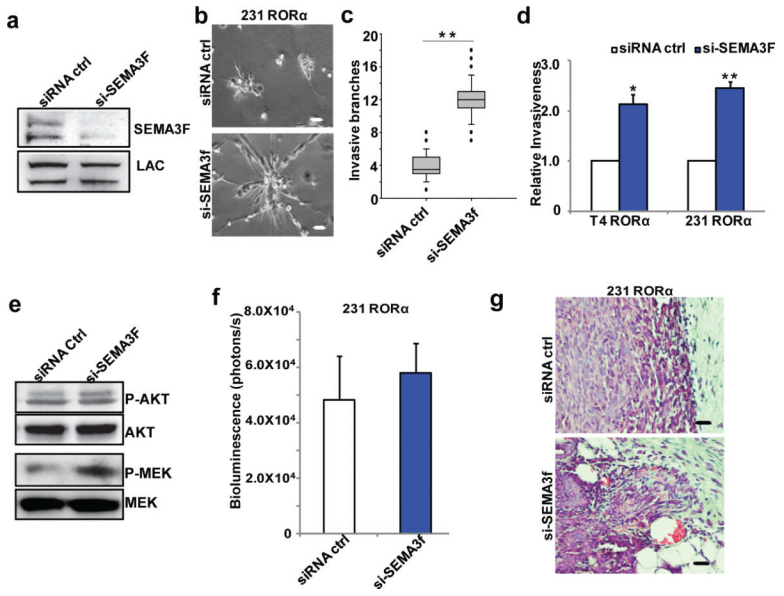

Fig 6.

Silencing SEMA3F partially rescues the malignant phenotypes suppressed by RORα. (a) Western blot results showed that SEMA3F protein level was reduced in si-SEMA3F transfected RORα-expressing breast cancer cells. (b) Phase images of control and SEMA3F-silenced RORα-expressing MDA-MB 231 cells in 3D culture. Silencing SEMA3F in RORα-expressing MDA-MB 231 cells rescued invasive phenotype of MDA-MB 231 cells in 3D culture. (c) Quantifying the invasive branches in siRNA control and SEMA3F-silenced RORα-expressing MDA-MB 231 cells. Over 40 colonies were counted, and the experiments were repeated three times. (d) Transwell assay showed that reducing SEMA3F expression in RORα-expressing T4-2 and MDA-MB 231 cells rescued the cell invasion, n=4. (e) Activation of Akt and MEK were assessed in the control and SEMA3F-silenced RORα-expressing MDA-MB 231 cells. Knockdown of SEMA3F enhanced phosphorylation of MEK. (f) Bar graph showing that silencing SEMA3F had little effects on tumor growth in RORα1-expressing MDA-MB 231/Luc cells. (g) Hematoxylin and eosin (H&E) staining of tumors formed by SEME3F knockdown and control RORα1-expressing MDA-MB 231/Luc cells. Bar: 20μm; * $p<0.05$, ** $p<0.01$.

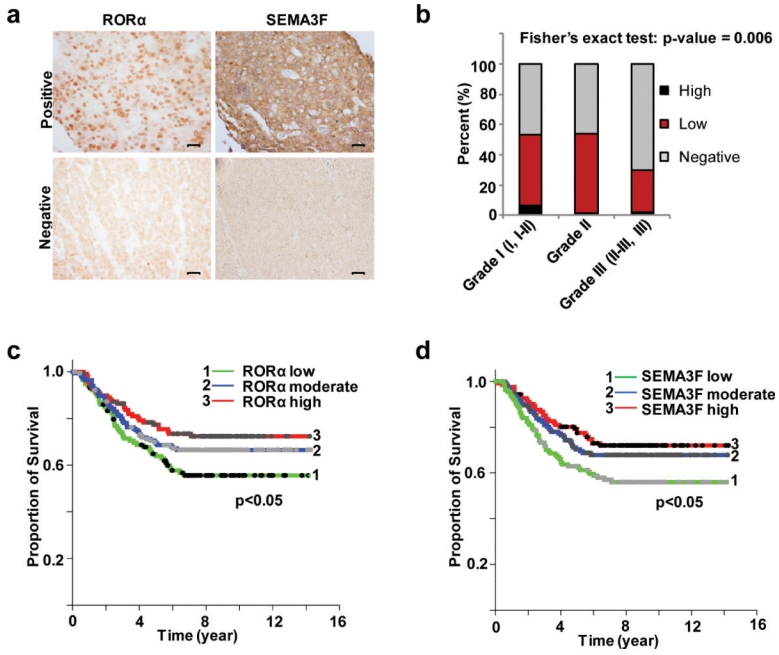

Fig 7.

Repression of RORα-SEMA3F pathway is associated with poor prognosis in breast cancer patients. (a) IHC analysis of RORα and SEMA3F expression in human breast cancer tissue array. Bar: 20μm. (b) Bar graph showing that the distribution of double positive or negative staining of RORα and SEMA3F in grad I, II and III breast tumor tissues. The Fisher's exact test showed that inactivation of RORα and SEMA3F is associated with high tumor grading (see Supplemental Table 2). (c, d) Kaplan Meier survival analysis of breast cancer patients grouped by expression levels of RORα (c) and SEMA3F (d). The tumor samples were classified into low (RORα, n=114; SEMA3F, n=131), high (RORα, n=121; SEMA3F, n=124), and moderate (RORα, n=169; SEMA3F, n=149) based on the mRNA levels of RORα or SEMA3F in the published microarray datasets. Significant differences in survival time were calculated using the Cox proportional hazard (log-rank) test.

Table 1

Correlated Expression of ROR and SEMA3F in human breast cancer tissues.

RORA\SEMA3F	High (++)	Low (+)	Negative (−)
High (++)	5	3	2
Low (+)	8	72	32
Negative (−)	2	14	105
Fisher's exact test p-value =2.20e-16			

A table summarizing the IHC staining of RORα and SEMA3F in human breast cancer tissues. The staining intensity of SEMA3F and RORα was graded to three different levels. The Fisher's exact test showed that nuclear levels of RORα significantly correlate with SEMA3F expression.